AD-A082 325 FOREIGN TECHNOLOGY DIV WRIGHT-PATTERSON AFB OH F/G 11/6
HARDENING OF STEEL WITH HIGH-SPEED DEFORMATION IN WIDE TEMPERAT--ETC(U)
FEB 80 L I MIRKIN
UNCLASSIFIED FTD-ID(RS)T-0231-80 NL

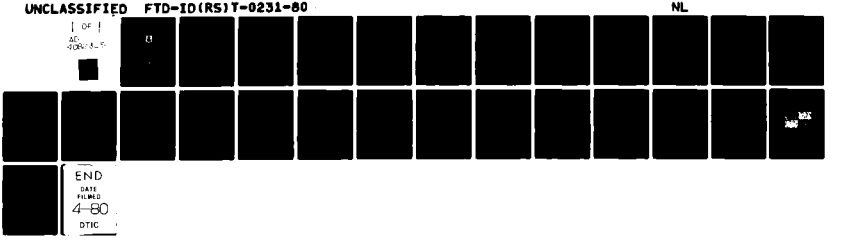

END
DATE FILMED
4-80
DTIC

FTD-ID(RS)T-0231-80

FOREIGN TECHNOLOGY DIVISION

HARDENING OF STEEL WITH HIGH-SPEED DEFORMATION IN WIDE TEMPERATURE RANGE

By

L. I. Mirkin

Approved for public release;
distribution unlimited.

80 3 24 025

EDITED TRANSLATION

(14) FTD-ID(RS)T-0231-80 (11) 28 Feb [redacted] 80 (12) 27

MICROFICHE NR: FTD-80-C-000274

(6) HARDENING OF STEEL WITH HIGH-SPEED DEFORMATION IN WIDE TEMPERATURE RANGE,

By: L. I. Mirkin (10)

English pages: 24

(21) Edited trans. of

Source: Fizika i Khimiya Obrabotki Materialov (USSR) [redacted] p105-113 + 1967, by

Country of Origin: [redacted]

Translated by: Marilyn Olaechea.

Requester: FTD/TQTD

Approved for public release; distribution unlimited.

PREPARED BY:

TRANSLATION DIVISION
FOREIGN TECHNOLOGY DIVISION
WP-AFB, OHIO.

141600

U. S. BOARD ON GEOGRAPHIC NAMES TRANSLITERATION SYSTEM

Block	Italic	Transliteration	Block	Italic	Transliteration
А а	*А а*	A, a	Р р	*Р р*	R, r
Б б	*Б б*	B, b	С с	*С с*	S, s
В в	*В в*	V, v	Т т	*Т т*	T, t
Г г	*Г г*	G, g	У у	*У у*	U, u
Д д	*Д д*	D, d	Ф ф	*Ф ф*	F, f
Е е	*Е е*	Ye, ye; E, e*	Х х	*Х х*	Kh, kh
Ж ж	*Ж ж*	Zh, zh	Ц ц	*Ц ц*	Ts, ts
З з	*З з*	Z, z	Ч ч	*Ч ч*	Ch, ch
И и	*И и*	I, i	Ш ш	*Ш ш*	Sh, sh
Й й	*Й й*	Y, y	Щ щ	*Щ щ*	Shch, shch
К к	*К к*	K, k	Ъ ъ	*Ъ ъ*	"
Л л	*Л л*	L, l	Ы ы	*Ы ы*	Y, y
М м	*М м*	M, m	Ь ь	*Ь ь*	'
Н н	*Н н*	N, n	Э э	*Э э*	E, e
О о	*О о*	O, o	Ю ю	*Ю ю*	Yu, yu
П п	*П п*	P, p	Я я	*Я я*	Ya, ya

*ye initially, after vowels, and after ъ, ь; e elsewhere.
When written as ё in Russian, transliterate as yё or ё.

RUSSIAN AND ENGLISH TRIGONOMETRIC FUNCTIONS

Russian	English	Russian	English	Russian	English
sin	sin	sh	sinh	arc sh	sinh^{-1}
cos	cos	ch	cosh	arc ch	cosh^{-1}
tg	tan	th	tanh	arc th	tanh^{-1}
ctg	cot	cth	coth	arc cth	coth^{-1}
sec	sec	sch	sech	arc sch	sech^{-1}
cosec	csc	csch	csch	arc csch	csch^{-1}

Russian	English
rot	curl
lg	log

HARDENING OF STEEL WITH HIGH-SPEED DEFORMATION IN WIDE TEMPERATURE RANGE

L.I. Mirkin (Moscow)

ABSTRACT. We know [1] that when metal specimens collide at relative speeds of 300-400 m/s plastic deformation and strengthening somewhat exceeding the corresponding values for static deformation are observed.

It has now become possible to conduct experiments at impact speeds which reach several thousand meters per second. Massive specimens of low-carbon steel 10 (0.1 o/o C) and technical iron (0.06o/o C) subjected to impact with an indentor at relative speeds in a range of from 1200 to 4000 m/s have been studied. Prior to impact the specimens were heated in a temperature range of up to + 700°C and cooled in a as low as -180° C. A number of experiments were also undertaken with specimens at room temperature.

To analyze results the investigation was conducted jointly with data published earlier for other types of pulsed hardening of analogous specimens (thermomechanical treatment with dynamic deformation [2]) hardening under the effect of light pulses from a laser [3], piercing of plates by an indentor, hardening by explosion, and the combined hardening effect of explosion and impact at high speeds [4].

As a result of the impact craters with approximately spherical surfaces were formed in the specimens.

In describing the effects an orthogonal coordinate system was used. The OZ axis was directed normal to the plane of the obstacle, while the OX and OY axes lay parallel to the plane of the obstalce and the origin of the coordinates was at the crater's apex.

The specimen was cut along the XOZ plane (in the middle of the crater) and deformation of the zone around the crater was studied.

A metallographic method was used along with X-ray diffraction analysis with photographic and ionization registration of intensity. Hardness distribution was measured and the deformation zone was estimated by a method of etching with various reactive agents. END ABSTRACT.

The findings were examined in the following order: a) constant rate of impact (1200 m/s), variable temperature of specimen (from -180° to + 700°JC), b) constant temperature of specimen (+ 20°C), variable speed of impact (from 1200 to 4000 m/s).

After low-temperature deformation curves for equal hardness around the crater section were plotted. Analysis of these curves shows that pulsed deformation causes hardess to increase from 110 to 170-175 Vickers units. Here the form of the isosklers reproduces very well the shape of the crater.

A metallographic study revealed that in the case of low-temperature deformation in the crater region a large number of twins form and grain deformation also occurs. Let us note a number of perculiarities in the twin structure for the case of low-temperature deformation under static conditions.

First, twins in the studied case were never continuous and always took the form of broken bands. Apparently several deformation waves had passed at different speeds through grains containing broken twins. The first wave at very high speed led to twinning deformation. The second, at lower velocity, led to the stardard homogeneous

deformation of the grain. In this case shear occured and the result was broken twins. The second peculiarity in the structure is the presence of bent twins (deformation band), which are rarely observed in static low-temperature deformation.

Note than in most grains twinning occurs in a single system. At the same time, in the presence of deformation from a plane explosion wave in the same steel two twinning systems in each grain are usually observed.

Figure 1 shows curves representing the change in dimensions of the grains along the coordinate axes. From this we learn that on the boundary of the crater the dimensions of the grains are definitely anisotropic. Under the effect of the shock wave the grain acquires a shape close to elliptical with the minor axis of the ellipse directed normal to the front of the shock wave. The dimensions of the grains in the direction of the OX axis change from 90 to 45 μm, in the direction of the OZ axis - from 20 to 40 μm, the ratio of grain axes exceeds 3.

It is interesting to compare these data with the results of analogous measurements when the target is at room temperature. In the latter case the limit values of grain dimensions along the OX and OZ axes were 60 and 25 μm, i.e., deformation of the grains was

significantly lower. From the deformation of grains it is possible to approximate the degree of deformation of the material by means of the Reshinger ratio [6]. Note that in this respect the possibility of mutual turning of the grains in the presence of plastic deformation has not been considered. However, as a special study conducted by I.M. Gryaznov [7] revealed, even in the presence of static deformation at low velocities, the percentage of mutual turning of the grains in low-carbon steel is still insignificant.

Calculation shows that the maximal degree of deformation at low-temperature impact was 230o/c. For comparison we might point out that after a deformation somewhat exceeds yield deformation an analogous calculation gives us a value of only 10 o/o. Deformation, in fact was even greater, since the calculations did not consider twinning effects.

To estimate the contribution of the twinning effect curves were plotted to represent the relative number of twins along the OZ axis. This curve is also shown in Fig. 1. From it we see learn more than 50c/o of the total number of twins lie within the limits of 1.5 mm of the apex of the crater. The twins are preserved even at a distance from the crater at which the dimensions of the grains cease to change.

This finding also appears to confirm the hypothesis of the passing of several deformation waves at different velocities and intensities. Waves at high velocity cause twinning processes; waves at low velocities cause grain deforation; damping of waves with high speed occurs at greater distances. It should be pointed out that, despite the high impact speeds, no softening effects, indicating heating of the crater surface, were observed.

An X-ray structural study with photographic registration of intensity revealed that the line on the X-ray photograph (for example, line (220) in the case of reverse photography with the emission of an iron anode) is solid at the crater's apex and somewhat expanded, but with distance narrows to a line characteristic for the X-ray pictures of annealed low-carbon steel.

Photography with ionization registration of the intensity and and rapid rotation of the specimen in its plane revealed that the effect of expansion of the line, even at great reflection angles, is not great. With the selected type of geometrical photographing conditions the width of the line (220) at the crater constitutes $13.5 \cdot 10^{-3}$ rad and $11.2 \cdot 10^{-3}$ at a distance of 16 mm from the crater. Estimation of the fine structural elements in the case of such small changes is unreliable.

When the collision is at room temperature (+20°C) a crater of somewhat greater depth is formed and the findings for grain dimensions and the number of twins in the crater qualitatively analogous to those presented above for the case of low-temperature deformation.

Sharp qualitative differences are observed in high-temperature (+700°C) deformation. Increasd hardness in the crater region in this case constitutes 90-100 kg/mm². The magnitude of the effect is greater here than it is for collisions at room temperature and a low temperatures (-180°C). In the crater region there is a rapid drop in hardness. With distance from the crater the pace of this decline in hardness slackens.

A metallographic study showed that in the material arcund the crater three clearly defined structural zones can be distinguished. On the crater surface is the zone of small equiaxial grains. The thickness of this zone along the OZ axis, i.e., at the bottom of the crater, constitutes 0.3 mm. Beyond it lies the zone of large grains which extend in a direction tangential to the surface of the crater. The thickness of this zone at the bottom of the crater is 1.5 mm. The third zone is that of equiaxial ferritic grains (original structure). The total thickness of the zone with the altered structure at the edges of the crater is approximately half that of the bottom.

The results obtained by measuring grain dimensions are presented in Fig. 2. From the diagram we learn that at the edge of the crater grain dimensions are small (about 10 μm) and equal in both directions. With distance from the crater's edge grain dimensions increase in both directions, although in the direction of the OX axis (tangential to the crater's surface) this increase is much more rapid than in the direction of OZ. As a result there develop extended grains with an axis ratio of approximately 3. After this the nonequiaxiality of the grains gradually decreases, and at a distance of about 3.5 mm from the crater there begins the original equiaxial structure with a grain size of about 30 μm.

In high-temperature deformation the twin formation characteristic of deformation under the same conditions at room and lower temperatures is not observed. If we compare the dimensions of the zones with altered microstructure with zones which have altered hardness, then we learn that the dimensions of the zone of altered hardness are significantly greather than those of the zone in which the microstructure has changed. The dimensions of the deformation zone obtained by macroetching coincide with those of the zone of increased hardness.

In X-ray photographs (irradiated area about 2mm²) taken in the undeformed region the Debye rings consist of individual spots indicating a large-grained structure. As we approach the crater the spots become blurred (5.5 mm from crater). This corresponds to the absence of visible changes in microstructure and an increase in hardness by 20 kg/mm² at a distance of 2.5 mm from the crater (zone of extended grains - hardness increased by kg/mm²). Along with the spots on the X-ray photographs a solid ring appears. Nearer the edge of the crater the lines on the Debye pictures appear in the form of blurred rings.

Registration of the X-ray pictures by the ionization method shows that in the region of the crater (up to 2.5 mm from the crater) there is a certain increase in the thickness of the lines on the pictures. An analysis of the elements of the fine crystal structrue revealed that in the region of the crater the dimensions of the blocks decline somewhat (from 1.5 to $1.8 \cdot 10^{-5}$cm) and the density of defects increases (from 0.8 to $1.5 \cdot 10^{10}$ cm^{-2}). This is almost within the limits of accuracy of the measurements. At the same time a significant increase is observed in microdistortions (from 0.03 to $0.06 \cdot 10^{-2}$), even though the absolute value of these microdistortions is not great. It should be noted that, as a result of the relatively large dimensions of the irradiated surface, these data refer also to the extended grains.

Thus, impact at high temperature apparently leads to the following effects. In the region directly adjacent to the crater's surface recrystallization occurs with the formation of small equiaxial crystals. The process is, in fact, even more complex than standard recrystallization, since the hardnes of this zone is significantly above that or the small-grained recrystallized ferrite.

At greater distances from the crater there is not sufficient energy for recrystallization during such a short time interval, and plastic deformation occurs. In this case plastic deformation occurs with only microdistortions and without noticeable crushing of the blocks. Finally, in a zone more distant yet from the crater only the properties of ferrite crystals change. Their form does not. One can anticipate that a sharp increase in the rate of impact will have the same effect as an increase in temperature.

Presented below are the findings for a specimen of technical iron after impact at a rate or 4000 m/s.

Macroetching of a crater section reveals three distinctly colored regions. Zones 1 and 3 (numbered from crater surface) are lighter than zone 2. Data of metallographic studies show sharp

differences in the structures of these zones. Photomicrographs of the characteristic zone regions are presented in Fig. 3.

Analysis of the photomicrographs shows that zone 1, which is nearest the crater, consists of approximately equiaxial grains, the grains at the very edge of the crater being somewhat larger. The following zone (zone 2), sharply demarcated from the first, consists of grains which extend in the direction tangential to the surface of the crater. Under high magnification we see that these grains have a structure reminiscent of fine twins.

With distance from the crater surface the ratio of the axes of extended grains decreases and very distirct twins appear in them. Here we frequently observe broken twins (zone 3). Still further from the crater surface the number of twins in equiaxial grains becomes even lower. No more than one twin system is observed in the grains, and there is a gradual transition to the original polygonal structure (zone 4).

We should mention here that zone 3, which contains twins, extends to a very great depth within the specimen. Whereas the thickness of zone 1 constitutes about 0.03 mm, and that of zone 2 equals 0.5, zone 3 extends to a depth of several centimeters. Inspection of a large area of the microscopic section shows that the

number of twins in the structure is somewhat greater than normal even at distances of about 10 cm from the crater.

The hardness of the original specimens was 160 kg/mm², and even in zone 1, containing equiaxial grains, hardness was 200 kg/mm², i.e., 40 kg/mm² above that of the original material. Very high hardness values were obtained in zone 2. The hardness of 380 kg/mm², revealed in this zone, is 220 kg/mm² higher than in the original material. Finally, in zone 3 hardness constitutes 239 kg/mm², i.e., it is 60 kg/mm² greater than in the original material.

The X-ray structural study, as one might expect, did not reveal any new phases in the region around the crater.

To study changes in dimensions and the orientation of crystals a method of azimuthal scanning of line (110) (Debye ring) was used. The technique used in analysis is described in [8]. In the case of a fine-grained structure, i.e., a large number of grains with random orientation in the irradiated volume of 0.5 X 0.05 mm, the curve representing the dependence of the intensity of reflectin from the azimuthal angle α should be horizontal. In the presence of texture in the material symmetrical maxima appear on this curve. Finally, in the case of large-grained structure with disordered orientation of crystals maxima which have no order should be observed. The results

of this registration are shown in Fig. 4.

As we learn from the diagrams representing the azimuthal involute of the intensity curve, in zone 1, which contains fine, equiaxial grains, the curve contains several more or less disordered maxima, i.e., the block structure is relatively fine and does not reveal any prevalent orientation. In zone 2 one can expect the appearance of distinct texture maxima and dips between them or, if a prevalent orientation is absent, the appearance of distinct but disordered maxima. The obtained curve is in fact characteristic of a specimen with very small crystal dimension and fine texture, i.e., the large grains visible in the photomicrograph are broken down into blocks.

Characteristic of zone 3 are maxima on the curve of the azimuthal involute and for zone 4 - increased height and distinctness of these maxima. Let us point out that even though the shapes and dimensions of the grains in zones 3 and 4 visible in the microscope are approximately identical, the appearance of twins leads to an increase in disorientation within the grain, as we learn from the X-ray photographs.

The dimensions of the blocks D (10^{-5} cm), the density of defects in the crystal lattice ρ (10^{10} cm^{-2}) and microdistortions Δ a/a were,

respectively, in zone 1 - > 5, < 0.1, < 0.01; in zone 2 - 1.2, 2.0, 0.05; in zone 3 - 1.4, 1.2, 0.02.

Here it should be mentioned that although the tendency toward change on the part of elements of the fine crystal structure coincides with the direction of changes in hardness, in absolute value the roentgen effects are comparatively small. Deformation of the iron (rolling with high degrees of reduction, for example) makes it possible to obtain more intensive crushing of the blocks and an increase in microdistortions and density of defects with substantially less increase in hardness. Apparently in static deformation and deformation by impact waves there are substantial differences in the form of the distribution of dislocations which cannot be detected from the expansion of the line in the X-ray photographs.

These results enable us to schematically represent processes which occur in iron under impact. Apparenlty at the the speed of impact employed (400 m/s) the release of energy at the moment of impact is so great that there occurs not only heat liberation sufficient for vaporization of part of the material and the development of a crater, but also a recrystallization in the thin surface layer as the result of the high temperature gradient in the remaining portion of the specimen.

The analysis of the microstructure of zone 1 discussed above shows that not only processing recrystallization occurs, but also partial collective recrystallization as well. This is followed by zone 2, which consists of deformed grains with a sound structure, internal distortions, and increased defect density. Here the existence of a very sharp boundary between the first and second zones, which points to a drastic change in temperature and pressure, will certainly be observed.

Finally, zone 3 has a structure usually obtained in dynamic or explosive deformation. A peculiarity of the structure in this case is the presence of one and sometimes two directions on the part of the twins in the grains, at the same time that deformation by explosion is characterized by the existance of 2-4 twin directions.

If we compare this with the deformation of a planar explosion wave, then we learn that according to the data of [9] and our data [4], right up to shock wave pressures of 550 kbar a microstructure characteristic of zone 3 (in our case) is observed. At the same time, in the presence of an intensive heat pulse from the light beam of a laser, as demonstrated in [5], by outward analogy with the effect of high-speed impact (formation of crater) the thermal effect is

significantly greater, and there develop secondary hardened structures characterized by a very high degree of hardness (up to 1500 kg/mm^2, for example for low-carbon steel).

With respect to the magnitude of energy released on the crater surface per unit time, the studied case is apparently intermediate between that observed at low impact speeds or the effect of plane shock waves with an intensity of less than 10^6 kbar and the effect of powerful light energy.

Qualitative explanations for hardening in the presence of the interaction between an indentor and a semi-infinite steel obstacle can be obtained on the basis of the Horntogen model [10], which was used earlier to analyze processes which occur in a shock wave. The main difficulty in describing the process lies not in explaning the development of dislocations upon passage of the shock wave, but in explaining the process of preservation of high dislocation density after removal of the load from the material.

The compressed regions of the crystal associated with dislocations lie within the compression wave, and density is equal to the difference between the volume inside and outside the shock wave.

It is assumed that dislocation loops form as the shock wave

passes through the crystals. The formation of a screw dislocation in each crystal during this process is illustrated by the diagram in Fig. 5.

It should be mentioned that the amplitude of the shock wave in the above experiments exceeded the value of the yield point by more than one order, since the deformation energy was quite sufficient for the formation of new dislocations.

An experimental study which employed a transmission type electron microscope [10] shows that the dislocations lie in two directions <111> in plane {110}, regardless of the orientation of the shock wave front in relation to that of the crystals. The boundary components of the dislocation loops in the diagram move at a speed approximating the speed of the shock wave front, since their compression zone (half-space) forms the zone of the compression wave. The helical components of the loops in this case remain in place, and their length increases as the boundary components pass through. The loss of energy in the wave is in this case proportional to the length of the screw portions of the dislocations.

From Fig. 5 we learn that the boundary components of the loops, which are inclined in relation to the shock wave front, move within the front, but in different directions. The Burgers vector of the

helical dislocations can be obtained by analyzing the position of the boundary dislocations in the shock wave front.

The helical dislocations which remain at the shock wave front may interact in two ways. The helical portions of the dislocations of the same loop have different signs and can be annihilated if they are too close. Helical dislocations lying within two different loops in a single plane of type [110] take the directions of the Burgers vector shown in Fig. 5. They can form nodes through the reaction:

$$\frac{1}{2}a[11\bar{1}]+\frac{1}{2}a[\bar{1}11]=a_{[010]}$$

It should be mentioned that the density of dislocations after the shock wave front has passed is not as great as might be expected in the individual volumes during compression of the material by shock waves. Therefore, both the reaction of loop compression and the reaction of node formation occur behind the shock wave front. Moreover, the studied model does not consider the change in behavior of disloactions at speeds approximating the speed of sound in the material.

Because of the increased probability of the development of packing defects under pulsed deformation it follows that the density of partial dislocations will also increase, i.e., that there will occur dissociation of total dislocations into partial. In this

respect we observe a similarity between deformation effects under thermomechanical hardening [11] and shock wave treatment. However all roentgen effects and hardening under thermomechanical treatment of steel of the same composition with the use of dynamic deformation at rates of 5 m/s and hardening [quenching] are higher than after shock wave deformation [2]. It should also be noted that the observed effects may have the same order as in the hardening [quenching] of steel and a somewhat higher order than in static deformation with high degrees of reduction.

Finally we must mention the fact that the source of softening of the material at very high deformation rates may be the existence of a limiting rate of movement on the part of the dislocations, above which, as demonstrated by A.A. Zhukhovitskiy and M.A. Krishtal [12], destruction, rather than hardening of the material, should occur. It appears that in all experiments described above the deformation rate considerably exceeds this limit value.

Conclusion. Low-temperature (-180°C deformation of low-carbon steel at impact speeds of 1200 m/s leads to the development of a spherical twin structure and grain deformation. High-temperature (+70°C) [sic] pulsed deformation provides additional recrystallization effects. Increasing the impact speed up to 4000 m/s at room temperature results qualitatively in the same pattern as

high-temperature deformation at low speed. The results of X-ray structural analysis and metallographic study of the deformed zone coincide with the dislocation models of shock wave effects on metal.

Received 20 January 1960.

References

1. Райнхарт Дж., Пирсон Дж. Поведение материалов при импульсивных нагрузках. Изд. иностр. лит., 1958.
2. Гольдер Ю. Г., Грязнов И. М., Крапивин Л. Л., Миркин Л. И. Сб. «Исследования по высокопрочным сплавам и нитевидным кристаллам». Изд. АН СССР, 1963, стр. 128.
3. Аверьянова Т. М., Миркин Л. И., Пилипецкий Н. Ф. Металловед. и термическая обработка металлов, 1966, № 4.
4. Козорезов К. И., Миркин Л. И. Докл. АН СССР, 1966, 171, № 2, стр. 324.
5. Аверьянова Т. М., Миркин Л. И., Пилипецкий Н. Ф. Ж. прикл. мех. и техн. физ., 1965, № 6 стр. 84.
6. Решингер В. А. Прикл. матем. и машиностроение, 1953, № 3, стр. 18.
7. Грязнов И. М. Докл. АН СССР, 1950, 126, № 6, стр. 1250.
8. Миркин Л. И. Физико-химическая механика материалов, 1965, № 6.
9. Дитер Г. Е. Сб. «Механизмы упрочнения твердых тел», Металлургия, 1965.
10. Hornbogen E. Acta metallurgica, 1962, 10, No. 10, p. 978.
11. Миркин Л. И. Сб. «Федоровская научная сессия. Тезисы докладов». Изд. АН СССР, 1962, стр. 129.
12. Жуховицкий А. А., Криштал М. А. Докл. АН СССР, 1963, 149, № 1, стр. 88.

Fig. 1. Distribution of grain dimensions d along OX axis (curve 1) and OZ axis (curve 2) and relative number of twins n along Z axis (curve 3) with distance from apex of crater in steel St. 10 (impact at -180°C, 1200 m/s). Key: μm, %.

Fig. 2. Distribution of grain dimensions in impact zone in steel St. 10 (impact at + 700°C, 1200 m/s): 1 - grain dimensions along OX; 2 - grain dimensions along OZ; 3 - ratio of grain dimensions X/Z along OX and OZ axes.

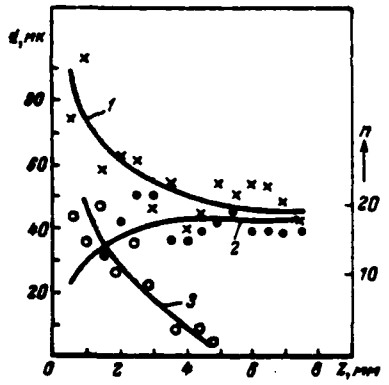

Fig. 1

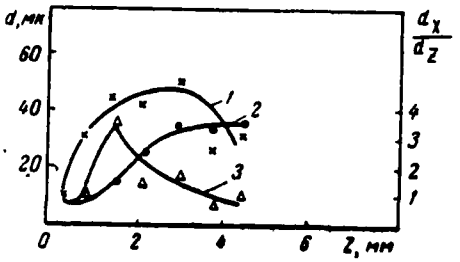

Fig. 2

Fig. 3. Microstructure of iron after impact at speed of 4000 m/s X 200: a - zone 1 of recrystallized grains; b - zone 2 of deformed grains with twins; c - zone 3 of equiaxial grains with twins; d - original structure (zore 4).

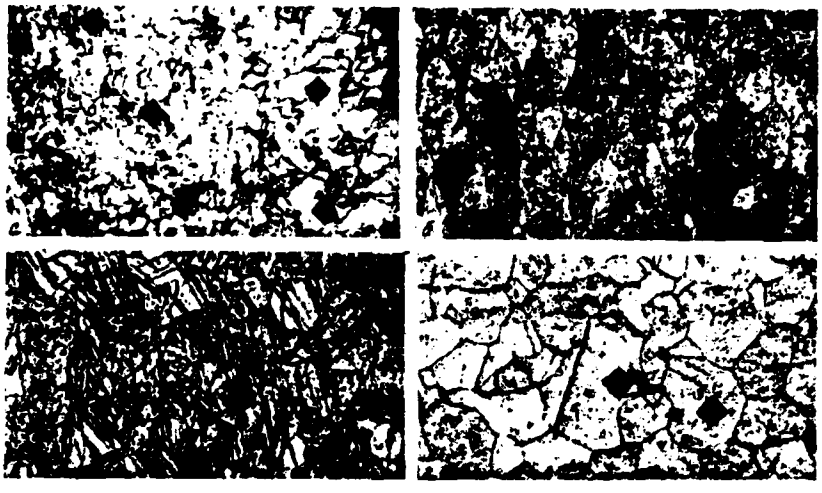

Fig. 4. Curves of azimuthal distribution of intensity of line (110) on roentgenograms of different zones in region of crater: a - zone 1 of recrystallized grains, b - zone 2 of deformed grains with twins, c - zone 3 of equiaxial grains with twins, d - original structure (zone 4).

Fig. 5. Diagram of dislocation formation in iron and steel during passage of shock compression wave: 1 - boundary components moving inside compression wave front, 2 - compression wave front moving in direction of [100], 3 - helical dislocations which remain behind compression wave front and lie in plane [101].

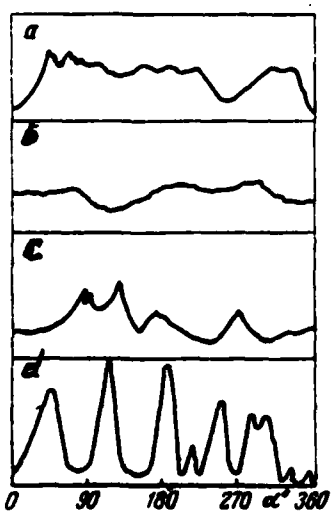

Fig. 4

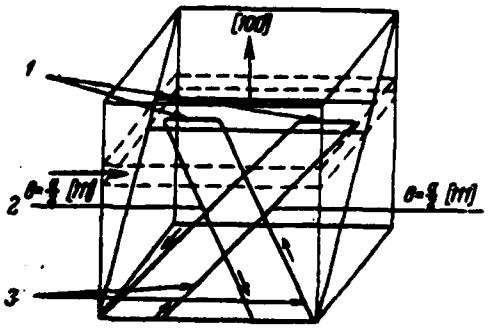

Fig. 5